

# Alignment experience in STAR

*S. Margetis<sup>a</sup>, Y. Fisyak<sup>b</sup>, J. Lauret<sup>b</sup>, V. Perevoztchikov<sup>b</sup>, G. Van Buren<sup>b</sup>, J. Bouchet<sup>c</sup>  
for the STAR Collaboration*

<sup>a</sup> *Kent State University, Kent, USA*

<sup>b</sup> *Brookhaven National Laboratory, New York, USA*

<sup>c</sup> *Subatech, Nantes, France*

## Abstract

The STAR experiment at RHIC uses four layers of silicon strip and silicon drift detectors for secondary vertex reconstruction. An attempt for a direct charm meson measurement put stringent requirements on alignment and calibration. We report on recent alignment and drift velocity calibration work performed on the inner silicon tracking system.

## 3.1 Introduction

The STAR experiment, with a similar layout to the ALICE LHC experiment, was primarily designed to detect signals of a possible phase transition in nuclear matter. Its layout, typical for a collider experiment, contains a large Time Projection Chamber (TPC) in a solenoid magnet, a set of silicon vertex detectors plus other detectors. In this report we will concentrate on alignment work performed on the central silicon tracker relative to TPC [1].

The physics motivation for this renewed effort has been the quest for a direct charm measurement, i.e., the identification of D-mesons from the reconstruction of their secondary decay vertices. This task is extremely difficult for a number of reasons, e.g., the short  $c\tau$  of the D decays coupled to the absence of significant Lorentz boost at mid-rapidity in a collider environment, inside a tracking environment of thousands of ‘background’ tracks, as in a typical Au+Au collision at  $\sqrt{s_{NN}} = 200$  GeV. Another reason is that the initial design goal for the central silicon tracker was to reconstruct secondary vertices from decays of multi-strange particles ( $\Xi$  and  $\Omega$  particles) with a  $c\tau$  of several centimetres and not charm decays. Thus the tracker was not optimized, in terms of thickness and distance from the interaction point, for this latter task.

STAR has a plan to upgrade its central silicon tracker using novel, ultra-thin silicon pixel detectors very close to the interaction point, for precise charm, and bottom, measurements. In the meantime, an alignment/calibration task force was formed in the fall of 2005 to explore the possibility of using the existing detectors for ‘some/any’ charm/bottom measurements.

This write-up is a progress report on our experience. It is our hope that the LHC groups might benefit from our experiences, good and bad.



**Fig. 3.1:** The fully assembled SVT detector (above). One can see the arrangement of the wafers in a ladder. The bottom part of the figure shows one (out of four total) SSD sector. The double-sided strip detectors are also arranged in ladders.

### 3.2 The silicon vertex complex

The central silicon tracker consists of three layers of silicon drift detectors encapsulated by a (fourth) layer of double-sided silicon strip detectors [2, 3]. Figure 3.1 shows the fully assembled SVT (above) and one SSD sector (below).

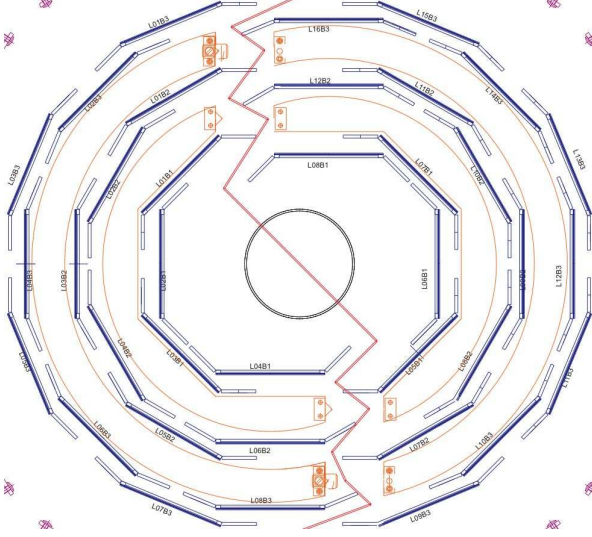


**Fig. 3.2:** The transverse layout of the SVT detector. The beam pipe and the left/right clam-shells are indicated. The darker lines are the SVT wafers. The little pieces on each side are electronic-components carriers. We see that each SVT layer is made out of two sub-layers.

The SVT is the first full-scale detector using this particular technology while the SSD was a first-generation full-scale prototype of the ALICE strip detector. The average distances of the three SVT layers from the primary vertex are 7, 11 and 15 cm (Fig. 3.2). The silicon drift wafers are arranged in ladders which are attached to two hemispheres or ‘clam-shells’ that wrap around the beam pipe (see also Fig. 3.2).

The SSD layer is at an average distance of 23 cm from the vertex. Its main purpose is to serve as a track ‘matcher’, i.e., connect the TPC tracks to the SVT points. For reference, the TPC inner field cage starts at 50 cm and the first active pad-row is at 60 cm from the primary vertex. The SSD double-sided strip wafers are also arranged in ladders which are attached to four ‘sectors’ which surround the SVT. The non-drifting technology of the SSD provided an invaluable reference in this alignment/calibration task.

One of the critical parameters that affects the overall detector pointing accuracy is the average thickness of each SVT layer. Although the wafer thickness is  $0.3\% X_0$  (for  $300 \mu\text{m}$ -thick silicon), the overall support-/electronics/cooling assembly has an average radiation

thickness of about  $1.5\% X_0$  per layer. This thickness coupled to the 7 cm distance of the first SVT layer from the interaction region leads to a minimum track DCA (or track impact parameter) resolution in the transverse direction, at the primary vertex, of about  $140 \mu\text{m}/(\text{GeV}/c)$ . This multiple Coulomb scattering (MCS) limit defines the goals of our alignment and drift velocity calibration effort, i.e., we should keep their combined errors below about  $80 \mu\text{m}$ . One needs to remember the presence of non-Gaussian tails in the MCS distribution at the 2% level.

In the presence of thousands of tracks, impact parameter alone is not sufficient. One also needs high track reconstruction efficiency with low ghost rates and therefore the relative fine-tuning of all detectors involved in tracking (TPC+SSD+SVT) is crucial. This fine-tuning also requires high quality alignment.

### 3.3 The alignment model

Our calibration sample consists of 250 000 Cu+Cu events taken at  $\sqrt{s_{NN}} = 62 \text{ GeV}$  beam energy. The sample was taken during Run-5 in 2005. This was the first physics run with both sets of central detectors (SSD+SVT) fully deployed. We chose runs at the end of the collider fill time so that we get the lowest possible luminosity, in order to minimize space-charge effects (distortions) in the TPC. This is an important point one needs to remember when choosing an alignment sample.

Our approach was to follow as closely as possible the physical model of the detectors. Our plan has three steps of which the first two are in quite advanced stages while the third is in progress:

- Global alignment
- SVT drift velocity calibration
- SVT self alignment

During the global alignment step, we first focused on aligning the SSD sectors and SVT clam-shells using TPC track information only, i.e., we did not include the SSD/SVT hit information on the track fit. An iterative, global parameter minimization approach was used. Our alignment methods were initially checked with Monte Carlo techniques and at the end, the figure of merit was the improved mass resolution and reconstruction efficiency of, e.g., strange particles like  $K$  and  $\Lambda$ .

After the SSD sectors and SVT shells were positioned inside the TPC track footprint, fine-tuning of the individual SSD ladder positions was performed. At the completion of this step, the SSD geometry was frozen and the combined tracking of both TPC+SSD was used to fine-tune the SVT ladders (in the non-drifting z-direction) and also calibrate the SVT drift velocities. At the end the SVT ladders were re-tuned using the whole tracking information (TPC+SSD+SVT).

The starting geometry point was optical survey measurements on the assembly bench of a) the ladders on the shells/sectors (estimated accuracy of about 20-30  $\mu\text{m}$ ) and, b) the wafers on the ladders. The latter measurements, performed using a high resolution camera, have an estimated error of a micron and therefore the individual wafer position on the ladder was frozen, i.e., the lowest degree of freedom touched by our procedure was the ladder, not individual wafers.

Only primary tracks (i.e., tracks successfully fitted with the primary vertex hypothesis) were used throughout this alignment process. Typically, about half the total number of tracks in an event end up as primary tracks.

We do not have any successful self-alignment method so far to report here, and this is still a work in progress [4].

Notations: global coordinates are X, Y, Z. Local wafer coordinates are  $u = x$  (drift),  $v = z$  (beam),  $w = y$  (normal to wafer plane) and  $\alpha, \beta, \gamma$  are rotations around  $u, v, w$  or global X,Y,Z, respectively. The units are cm and mrad. Note that the rotations have different actual orientation in local and global coordinates.

The ‘rigid body’ model has been applied (i.e., we ignored possible ladder twist and sagging effects for the moment). We introduced a typical misalignment model, e.g., the D0 experiment alignment model [5]. We performed a Taylor expansion with respect to misalignment parameters (3-D shifts ( $\Delta u, \Delta v, \Delta w$ ) and 3-D rotations ( $\Delta\alpha, \Delta\beta, \Delta\gamma$ )) for deviations of measured hit position from predicted primary track position on a measurement (wafer) plane. The track prediction comes from the detector(s) used as reference, e.g., initially the TPC alone, and later the combined TPC+SSD tracking. In the next step, from the hit deviations distribution, a misalignment parameter has been calculated as a slope with a straight line fit (see examples below). As we mentioned earlier, a global least-squares fit was simultaneously performed on all available information. The method was applied iteratively until the fitted parameters reached stability.

### 3.3.1 Global SSD and SVT alignment using survey and TPC tracks

At this step only TPC tracking information was used as a ‘prediction’ in order to form the hit residuals. It was assumed that, on the average, any distortion effects cancel out. This hypothesis served us well in our calibration sample of Cu+Cu 62 GeV.

The fact remains that the TPC is a drift detector itself and this can cause some instabilities in alignment. For example, when we first applied the 62 GeV calibration constants to the Cu+Cu 200 GeV data, taken during the same run period, some systematic shifts of the silicon detectors were observed. These shifts showed dependencies on the magnetic field settings (zero field, full

field or reverse full field), which could not be explained as TPC distortions and implied actual relative movement of the detectors. At the same time, there are indications that during these runs, further tuning/adjustment of the TPC drift velocities and  $t_0$  (the effective time elapsed from trigger to the start of reading-out the detector) are necessary. These adjustments are of the order of a couple of hundred microns and they were impossible to detect without the help of the precision silicon detectors. Unfortunately, there is no hardware monitoring of the relative positions of the detectors in-situ, and therefore this has to be determined and monitored with software. As a direct result of these studies, a new alignment level was introduced and it deals with the relative position of the SSD+SVT cone assembly, as a whole, to the TPC. Since this is work in progress and only relevant to the 200 GeV data set, we will not go into any details here.

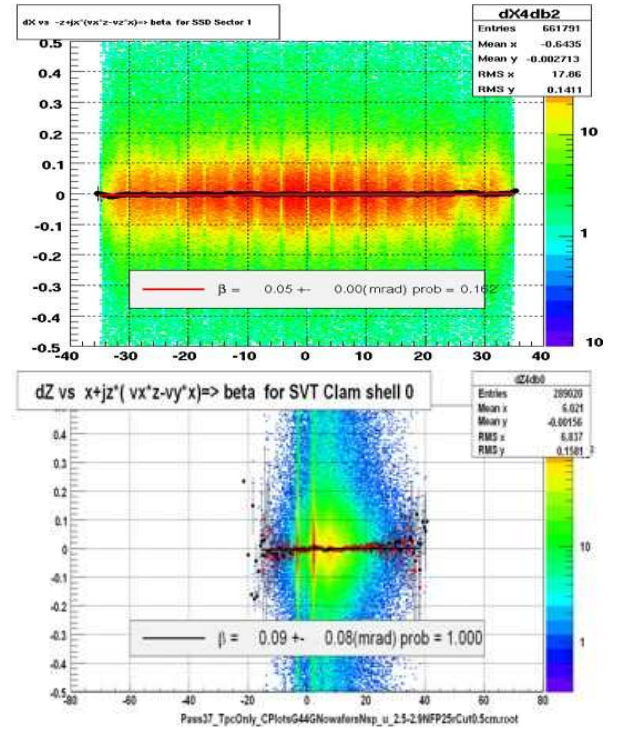


Fig. 3.3: Examples of fit results for global rotations for the SSD sector-1(above) and SVT clam-shell-0 (below). This particular parameter ( $\beta$ ) is the rotation of the sectors/shells around the global Y-axis.

#### 3.3.1.1 Global SSD sector and SVT clam-shell alignment

The SVT clam-shells and SSD sectors were aligned using only TPC tracking information (see Fig. 3.3). The SVT and SSD ladder survey geometry was assumed at this point. As we mentioned earlier, the ladder-on-shell accuracy of the survey data is estimated (hardware/software) to be around 20–30  $\mu\text{m}$ .



Proper math for global shifts/rotations was developed (same procedure as in local) but for rigid, non-planar objects in global coordinates. It was checked for accuracy and limitations with Monte Carlo blind tests which showed that it can be used in global alignment to better than 20–30  $\mu\text{m}$  accuracy for translations and about 0.1 mrad for rotations.

In order to minimize drift velocity miscalibration effects in the SVT, only the first 4 mm of drift around the anodes were used ( $|\text{l}|$  in the range of [2.5,2.9] cm out of [0.0,3.0] cm total drift distance). We also excluded 1 mm around the readout anodes due to variations in the focusing electric fields surrounding the anodes.

When this alignment step was performed to our satisfaction, most shells/sectors were (on average) aligned to better than 50  $\mu\text{m}$  in translations, and better than one mrad in rotations.

### 3.3.1.2 SSD ladder tuning

Some ladders showed relative translations within the same sector of up to 200  $\mu\text{m}$  and rotations (especially around y-axis) of up to 20 mrad. A fine-tuning was performed. The resulting alignment constants replaced the original optical survey measurements. In the SSD case, this is justified since some survey parameters, especially related to rotations, were poorly determined due to survey equipment limitations. Also, software alignment determines the position of ladders in-situ, taking into account possible installation distortions. After the SSD ladder fine-tuning was finished, the majority had translations of less than 20  $\mu\text{m}$  and rotations of less than 0.5 mrad, all within estimated errors.

After this step, the SSD geometry was frozen and the SSD hits were added to TPC tracks with proper errors. In this particular case, we used the errors of the design specifications of the detector which are 30  $\mu\text{m}$  in  $R\Phi$  and 700  $\mu\text{m}$  in the Z direction.

### 3.3.1.3 SVT tuning using TPC+SSD combined tracking

In the next step, the combined TPC+SSD tracks were used to tune the SVT. This contains several tasks. The first is to check/redo the SVT clam-shell global positioning. The second task is the fine-tuning of the SVT ladders in the non-drifting (Z) direction. Individual ladders showed Z-translations up to 400  $\mu\text{m}$  (but the bulk was around  $\pm 100 \mu\text{m}$ ). We believe that this discrepancy between survey and in-situ positions is due to work done on shells after the survey was completed (due to a water leakage in the detector). Also, two SVT ladders were replaced and serviced after the initial survey. Touching the detector after the survey is done should be avoided! At this point, only the beam (Z) direction was fine-tuned,

since this represents the anode, or non-drifting, direction of the SVT. After this SVT ladder fine-tuning the majority showed translations of less than 20  $\mu\text{m}$  and an example of this procedure is shown in Fig. 3.4.

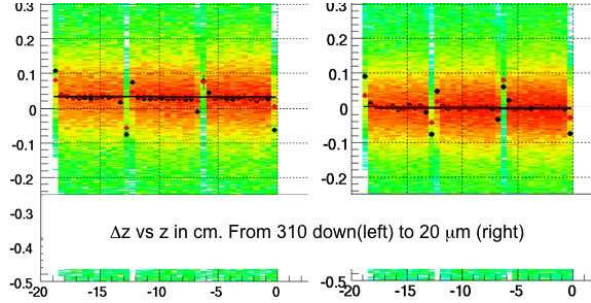


Fig. 3.4: Tuning of the z-position of an SVT ladder inside the clam-shell.

The third task is only indirectly related to alignment and it is related to the calibration of the individual SVT hybrid's drift velocity. This is discussed in the following section.

### 3.3.1.4 SVT drift velocity calibration using TPC and TPC+SSD information

The SVT hybrid calibration is a complex problem and we discuss it only peripherally here, i.e., only the alignment-related aspects of it. Each SVT wafer has two hybrids/two regions drifting in opposite directions [3]. This direction is the global transverse ( $R\Phi$ ) or bending direction. The drift velocity profile of a hybrid can exhibit variations in time. This is due to a variety of factors like temperature and voltage variations.

Like with any drift detector there are two characteristic quantities needed, the  $t_0$  and the drift velocity. For most of the drift region, the drift velocity can be assumed to be constant with some non-linear effects only around the anode region due to its focusing fields. For the calibration sample at 62 GeV, we started by using the default drift velocity parameters. As we can see in Fig. 3.5, the profiles exhibited an irregular shape.

This irregular shape (fortunately) remains stable in time, with the only exception of a couple of wafers. A fit with Chebyshev polynomials was performed in order to straighten the distributions in our calibration sample (insert in Fig. 3.5). The above was a quick fix that allowed us to proceed with our evaluation, but work has already begun to re-determine the drift characteristics of the hybrids, starting from the raw ADC vs time-bucket information. The 200 GeV data is about to be reprocessed with the new numbers in place.

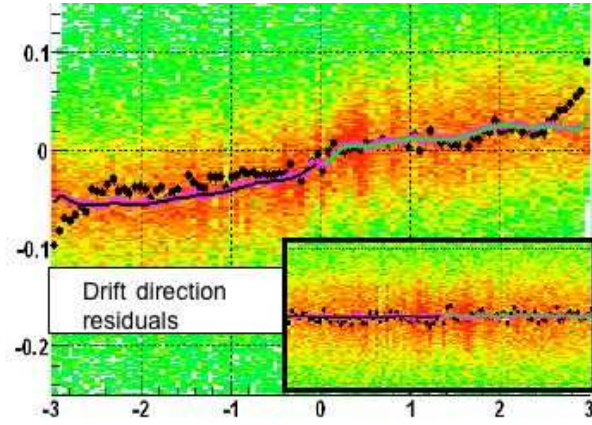


**Fig. 3.5:** Example of two SVT-hybrids (one wafer) drift velocity tuning.

### 3.3.2 Impact-parameter resolutions

The figure of merit for any alignment procedure is the DCA (track impact-parameter resolution from the event vertex), since it is this variable that allows the separation of the secondary vertices from the event vertex during physics analysis. In our case, the main factors determining the DCA resolution of the SVT/SSD (besides alignment and calibration) is the layer radiation thickness (multiple Coulomb scattering) and the distance of the first layer from the event vertex (lever arm).

The event vertex reconstruction resolution is also an important factor, but in our case (very high multiplicity), the expected resolution in central Au+Au events is not the limiting factor, as it is estimated to be well below  $50 \mu\text{m}$ .

The following figures show that we are close to the limits of the device, which indirectly shows that alignment/calibration errors do not dominate over the limiting MCS errors. Figure 3.6 shows the DCA resolution in the transverse (XY) direction for both simulation (top panel) and data (bottom).

Tracks without any SSD or SVT points (TPC only hits) are colored in red and labeled as ‘TPC’. In simulation, there are no such tracks since the SSD/SVT is 100% alive and therefore it is impossible for a primary track not to leave any SSD or SVT points. Only weak decays beyond the SSD with the decay tracks pointing back to the event vertex can give some spurious entries. In the data, this happens more often since several detector elements in the different layers are dead.

Tracks containing an SSD hit are coded in blue and labeled ‘SSD’. Finally, tracks with one, two or three SVT points are coded in green, red and black. The plot shows the r.m.s. of the full distribution as a function of inverse momentum, so infinite momentum corresponds to  $x \rightarrow 0$ .

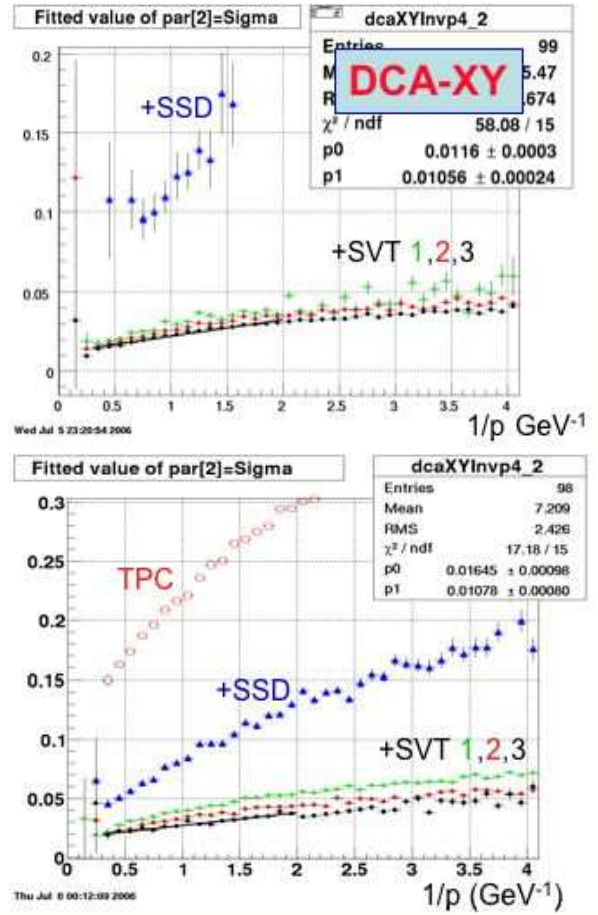


**Fig. 3.6:** Transverse impact parameter (DCA-XY) resolution for Hijing simulation (above) and data (below)

We should note that all quoted resolutions here include the event vertex resolution which is not an experimental observable. Also, the actual values are about 20% smaller than the quoted numbers due to the presence of non-Gaussian tails in the original distributions, which pull the r.m.s. to higher values.

The striking feature of these distributions is that the inclusion of even a single SVT point on the track makes a huge difference in terms of DCA resolution. This is mainly due to the closeness of the SVT to the event vertex (smaller lever arm). As we add more SVT points, the resolution slightly improves. At the infinite momentum limit (y-intersection of the distributions) the simulation shows a resolution of about  $120 \mu\text{m}$  whereas the data sample is about  $160 \mu\text{m}$ , which hints that some residual alignment or calibration effects are still present. At a track momentum of  $1 \text{ GeV}$ , the corresponding values are about  $220$  and  $270 \mu\text{m}$ . These values are not far from the  $140 \mu\text{m}$  value for the pure multiple scattering term, if one accounts for the additional event vertex and hit resolution errors.

Figure 3.7 shows the same distributions in the non-bending (Z) direction for both simulation (top) and data (bottom). At the infinite momentum limit, this non-drifting direction shows in simulation a resolution of about  $70 \mu\text{m}$  whereas the data sample is about  $80 \mu\text{m}$ . These numbers are consistent with the event vertex resolution in this sample and show a robust alignment result in the absence of drift velocity complications. Again, at a track momentum of 1 GeV, the corresponding values are about  $160 \mu\text{m}$  and  $170 \mu\text{m}$ , which are directly comparable to the scattering limit if one includes the vertex resolution. These results, especially the ones in the non-drifting direction, make us feel confident in our alignment procedure.

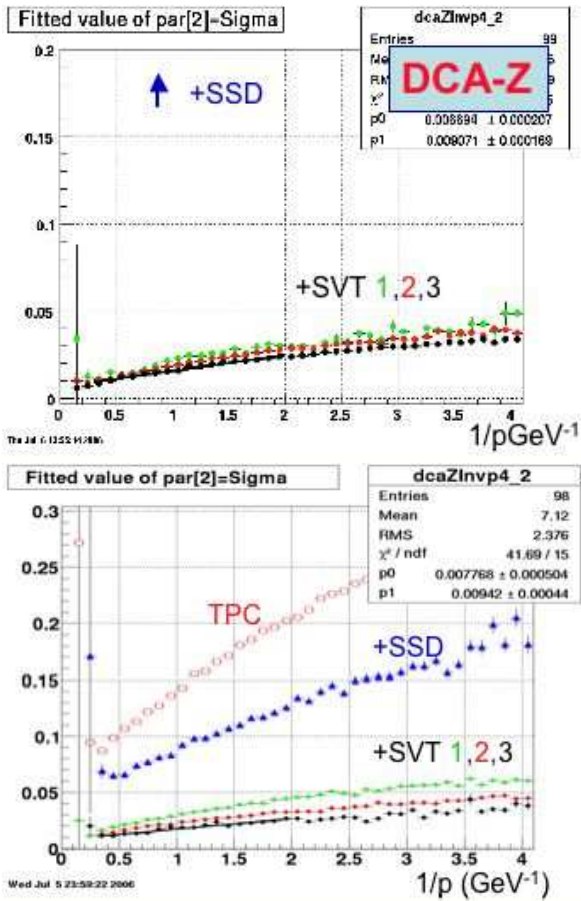


**Fig. 3.7:** Non-bending plane impact parameter (DCA-Z) resolution for Hijing simulation (above) and data (below)

### 3.4 Summary

Recent interest in charm physics re-focused STAR's interest in its vertex detectors, exploring the possibil-

ity of a direct charm measurement using the existing SSD+SVT silicon tracker. We found that silicon drift technology complicates the task of alignment, and therefore the use of non-drifting detectors (strips or pixels) will prove invaluable.

Our global alignment approach and techniques were successful to overall shifts better than  $20 \mu\text{m}$ , which for this device is sufficient. We realize that a lot of effort is still needed in order to understand and calibrate the TPC to resolutions appropriate to our alignment effort. In turn, we firmly believe that a well-aligned central tracking system could become a high-resolution device to undo many TPC distortions caused by a variety of sources.

Our self-alignment methods are still under development. We believe that the remaining shortcomings are a combination of poor error understanding and lack of sufficient ladder overlap, and not an intrinsic problem of the method.

The STAR experiment has an aggressive upgrade programme and our current work and experience might prove invaluable in future efforts.

### Acknowledgements

We wish to thank D. Lynn and B. Soja for providing valuable survey data and advice. We are grateful to L. Martin for his invaluable work in SSD software. We are also thankful to M. Potekhin for providing the misaligned Monte Carlo sample and M. Munhoz, H. Caines and R. Witt for their advice in numerous discussions. And last, but not least, we would like to thank the organizers of this important workshop.

### References

- [1] M. Anderson *et al.*, *Nucl. Instrum. Methods* **A499** (2003) 659.
- [2] L. Arnold *et al.*, *Nucl. Instrum. Methods* **A499** (2003) 652.
- [3] R. Bellwied *et al.*, *Nucl. Instrum. Methods* **A499** (2003) 640.
- [4] G. Van Buren *et al.*, <http://www.star.bnl.gov/STAR/comp/calib/SVTAlignment/SVTSmallScaleSelfAlignment.pdf>
- [5] D. Chakraborty and J.D. Hobbs, <http://d0server1.fnal.gov/projects/OfflineCalibAlign/docs/alignment/smtbar01.ps>